

Supporting Information

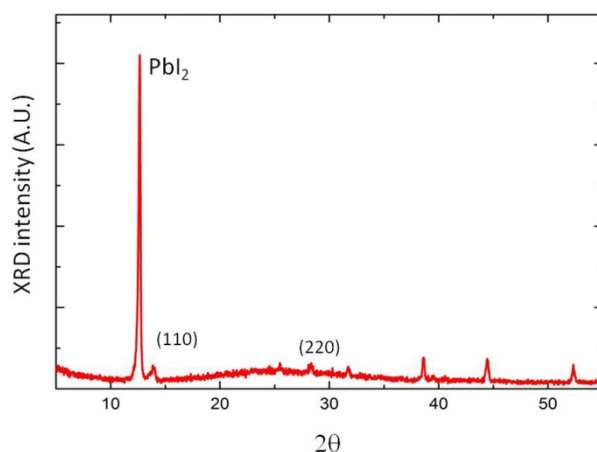
High Performance Perovskite Solar Cells by Hybrid Chemical Vapor Deposition

Matthew R. Leyden, Luis K. Ono, Sonia R. Raga, Yuichi Kato,

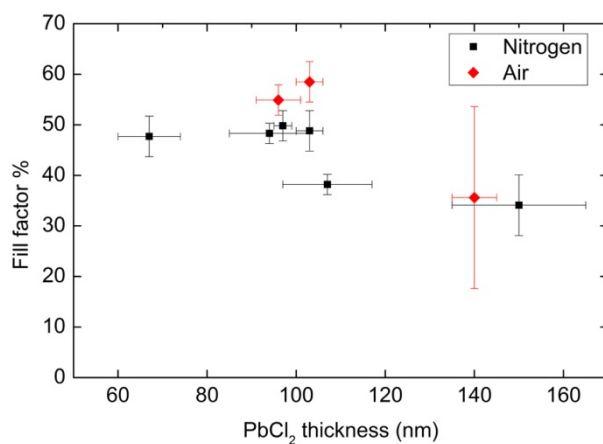
*Shenghao Wang, and Yabing Qi**

Energy Materials and Surface Sciences Unit, Okinawa Institute of Science and Technology Graduate University, 1919-1 Tancha, Onna-son, Okinawa, 904-0495, Japan

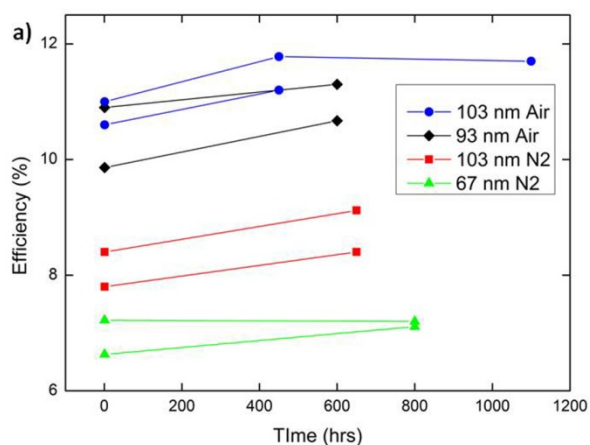
* Corresponding author: yabing.qi@oist.jp



Supporting Figure 1. X-ray diffraction spectrum of yellow film formed from PbCl_2 at high temperatures. The yellow color of the film and the XRD spectrum with a strong peak at 12.6° reveals that the film is PbI_2 and not perovskite. As deposited PbCl_2 is amorphous as does not produce XRD peaks. This amorphous nature of PbCl_2 contributes to more uniform thin films.



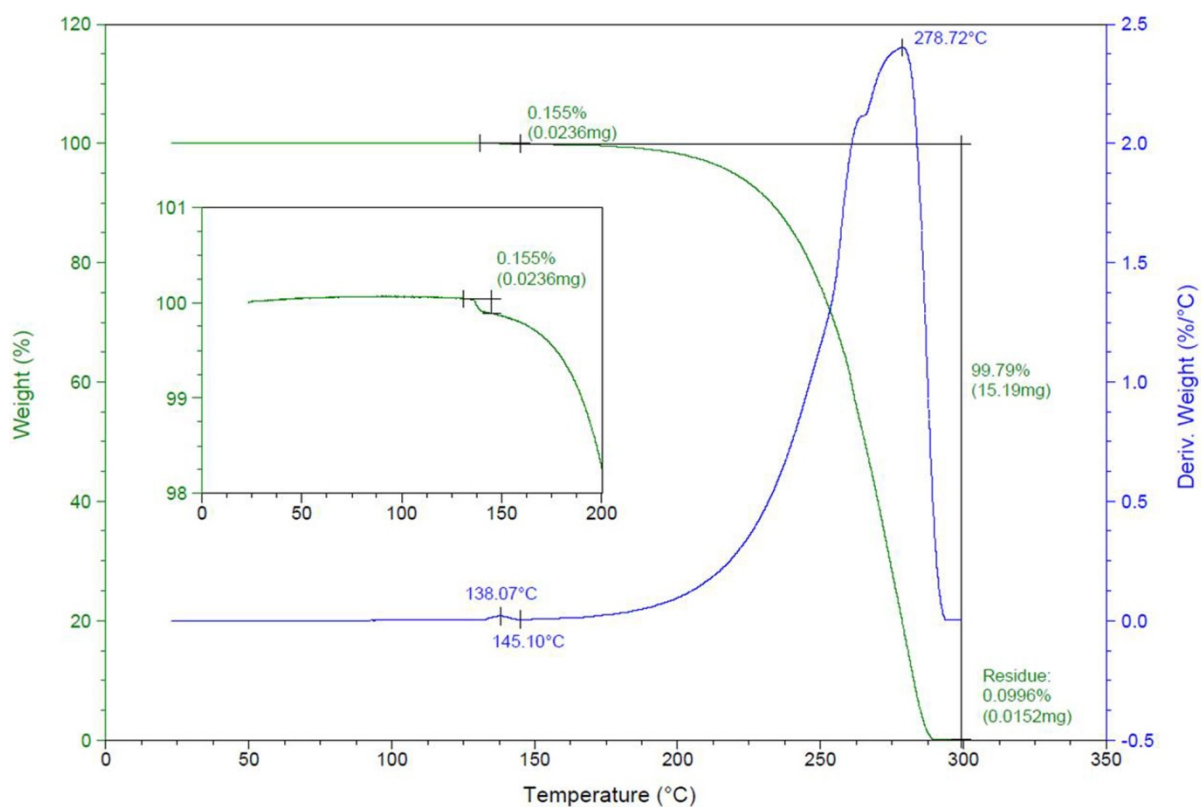
Supporting Figure 2. Fill factor as a function of PbCl_2 thickness. The fill factor is observed to go down with increasing thickness, which is believed to be due to low hole mobilities of the electron blocking layer or perovskite grain sizes smaller than the film thickness.



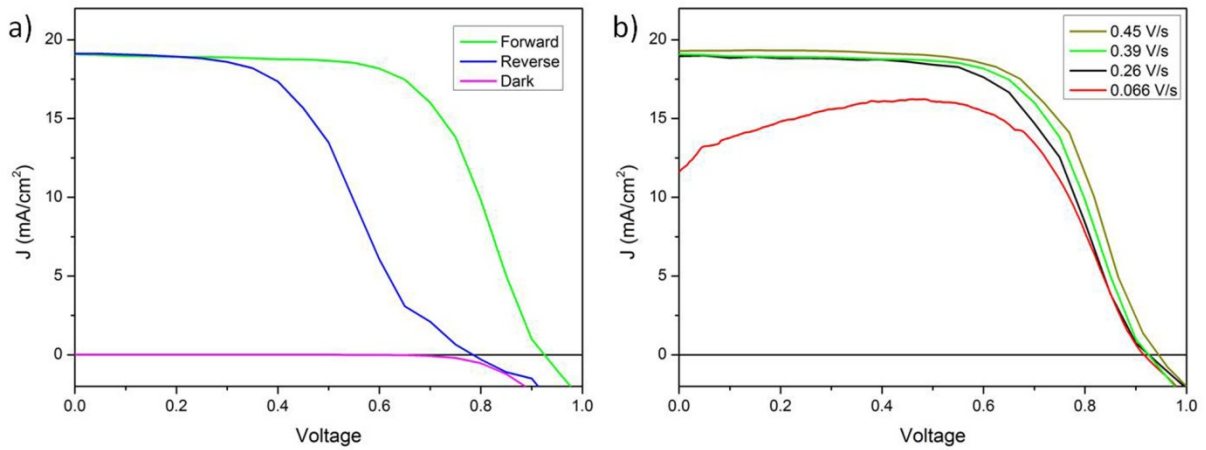
b)

| Sample | PCE % ~1 hr | PCE % 450 hrs or more | % change |
|-------------------|----------------|--------------------------|----------|
| 67 nm N2 anneal | 4.7 +/- 2.3 | 6.3 +/- 1.4 | 25 |
| 93 nm Air anneal | 9.5 +/- 1.3 | 8.6 +/- 2.5 | -10 |
| 103 nm N2 anneal | 6.1 +/- 2.1 | 6.9 +/- 1.6 | 12 |
| 103 nm Air anneal | 10.7 +/- 0.9 | 10.8 +/- 0.7 | 1 |
| | | average % change | 7 |

Supporting Figure 3. Stability of perovskite solar cells stored in a N₂ glove box. **a)** Stability graph of the top two performing devices of representative batches with different thicknesses and annealing conditions. **b)** Average performance of 4 representative batches of 6 devices. Most devices measured performed as well as or better than the original measurement.



Supporting Figure 4. Thermogravimetric analysis was performed on methylammonium iodide by TA instruments. This shows that MAI mass loss begins to happen at 145 °C. This is consistent with the observation that perovskite films formed by HCVD with a maximum temperature of 145 °C and below have excess MAI, and therefore degrade more rapidly.



Supporting Figure 5. Device performance under different measurement conditions. a) Shows the forward, reverse, and dark current measurements. b) Measurement as a function of sweep speed. The dark yellow curve was measured 7 weeks after fabrication and is the highest performing curve. This illustrates that the performance does not quickly decay if stored in N₂, and performance depends more on sweep speed than age. This curve has an average sweep rate of 0.45 V/s with 5 ms dwell time and 30 measured points. All other curves were measured at 3 weeks age. The green curve has an average sweep rate of 0.39 V/s with 5 ms dwell time and 25 points. The black curve has an average sweep rate of 0.26 V/s with 50 ms dwell time and 25 points. The red curve has an average sweep rate of 0.066 V/s with 5 ms dwell time and 250 points. All measurements were performed with 90 s or more of illumination prior to sweeping the voltage. Pre-illumination was found to be important for consistent performance. Pre-illumination times longer than 90 s were not found to improve performance. ¹

| Nitrogen annealed | | | | |
|----------------------------------|-----------------|------------------------------------|-------------|------------|
| PbCl ₂ thickness (nm) | V _{oc} | J _{sc} mA/cm ² | Fill Factor | Efficiency |
| 67 | 0.66 | 14.4 | 47 | 4.7 |
| 94 | 0.91 | 18.5 | 48 | 8.1 |
| 97 | 0.81 | 18.2 | 50 | 7.3 |
| 103 | 0.82 | 17.2 | 50 | 7 |
| 107 | 0.68 | 18.0 | 38 | 4.8 |
| 150 | 0.8 | 14.4 | 34 | 3.9 |

| Air annealed | | | | |
|----------------------------------|-----------------|------------------------------------|-------------|------------|
| PbCl ₂ thickness (nm) | V _{oc} | J _{sc} mA/cm ² | Fill Factor | Efficiency |
| 96 | 0.89 | 19.9 | 54 | 9.5 |
| 103 | 0.92 | 19.1 | 62 | 10.8 |
| 138 | 0.89 | 16.1 | 36 | 5.7 |

Supporting Figure 6. Summary of average device performance with different PbCl₂ thickness and annealing conditions.

Experimental

MAI was synthesized in a process similar to literature.² A hydroiodic acid solution was gradually added to methyl amine ethanol solution and kept stirring in an ice-bath. Ethanol and water from the solution was evaporated using a rotary evaporator (BUCHI, Rotavapor R-3). The precipitated yellow-colored crystals were dissolved in hot ethanol, and cooled in a refrigerator at 5 °C for recrystallization. Subsequently, the crystals were filtered and washed with tetrahydrofuran resulting in white crystal powder. We dried and kept the MAI in N₂ glove box (<0.1 ppm of O₂ and H₂O). FTO glass (Pilkington, 7 Ω/□) was patterned by etching with Zn powder and HCl 2M followed by brushing the surface with detergent, rinsing with deionized water and sonication in 2-propanol. A compact layer of TiO₂ was then deposited via spray pyrolysis using a precursor solution of acetylacetonate, Ti (IV) isopropoxyde and anhydrous ethanol (3:3:2) on a pre-heated hot plate at 480 °C. This layer was measured to be approximately 65 nm thick by profilometer (Bruker).

The PbCl₂ layer was deposited by thermal evaporation in a vacuum deposition system (~2.0 × 10⁻⁶ Torr), at approximately 0.5 Å/s, using PbCl₂ powder from Sigma-Aldrich. The thickness was monitored by a quartz-crystal microbalance and additionally measured using a profilometer.

Substrates pre-deposited with a PbCl₂ layer were loaded into the central zone of a multi-zone tube furnace (MTI 1200x III) and MAI is loaded into first zone. The furnace is then sealed and pumped down to a pressure of 100 Pa under the constant flow of N₂ gas. Substrates and MAI are ramped up to nominal temperatures of 130 °C, and 185 °C respectively over a period of 30 min and left at the intended temperatures for 1 h, and then are allowed to cool down to room temperature. After the substrates have been removed from the furnace they undergo a post annealing either on a hot plate at 120 °C in air or in a N₂ glove box.

The solar cell device fabrication was completed by spin-coating a hole transport layer that consists of a mixture of three materials: spiro-MeOTAD (2,2',7,7'-tetrakis(N,N-di-p-methoxy-phenylamine)-9,9'-spirobifluorene (Merck) dissolved in chlorobenzene (72.5 mg/mL), 17.5 μL of Li-bis (trifluoromethanesulfonyl) -imide (LiTFSI, Sigma) dissolved in acetonitrile (52 mg/100 μL), and 28.8 μL of tert-butylpyridine (*t*-BP, Sigma). Finally, the Au top electrodes were deposited by thermal evaporation (<1.0 × 10⁻⁶ Torr, at 0.1 Å/s) through a shadow mask defining solar cell active areas between 0.07 ~ 0.1 cm².

Current-voltage (i - V) characteristics of solar cells were measured under 1-sun illumination (AM 1.5G, 100 mW/cm²) using solar simulator (Newport Oriel Sol 1A) and a Keithley 2400 source meter. All measurements were performed without a mask and in ambient air with a temperature of ~25 °C and a relative humidity of ~50%.

All atomic force microscopy (AFM) measurements were performed using an Asylum instruments AFM and an AC mode cantilever with a nominal spring constant of 40 N/m. X-ray diffraction spectra were measured with a D8 Discover, Bruker Corporation. UV-vis transmittance spectrum was measured with an Evolution 600 spectrophotometer, Thermo Scientific.

References

1. U. B. Cappel, T. Daeneke, and U. Bach, *Nano Lett.*, 2012, **12**, 4925–4931.
2. M. M. Lee, J. Teuscher, T. Miyasaka, T. N. Murakami, and H. J. Snaith, *Science*, 2012, **338**, 643–647.